Atomistic Origin of Germanate Anomaly in GeO_2 and Na-Germanate Glasses: Insights from Two-Dimensional ^{17}O NMR and Quantum Chemical Calculations

Sung Keun Lee* and Bum Han Lee

Laboratory of Physics and Chemistry of Earth Materials, School of Earth and Environmental Sciences, Seoul National University, Seoul 151-742, Korea

Received: June 20, 2006

The prominent problem in archetypal germanate glasses is the *germanate anomaly* where the density exhibits maxima at 15−20 mol % of the alkali oxide content. Here we report ^{17}O two-dimensional NMR spectra for GeO_2 and Na-germanate glasses where the presence of both bridging oxygen linking $^{[4]}Ge$ and highly coordinated Ge ($^{[5,6]}Ge-O-^{[4]}Ge$) and nonbridging oxygen, and an increase in topological disorder are demonstrated at the density maximum, manifesting atomic origins of the anomaly. These densification mechanisms in germanate glasses with Na content are remarkably similar to densification in v-B_2O_3 with pressure.

1. Introduction

The structure of covalent oxide glasses is not well understood and thus establishing their structure−property relations is one of the unsolved questions in physical chemistry, condensed matter physics, and glass sciences.[1−4] Prototypical GeO_2 and alkali germanate glasses have been extensively studied due to their fundamental implications for the physics of multicomponent oxide glasses[5,6] and have applications as optical waveguides. Geophysically, germanates have been used to provide insight into the structures of silicates under extreme conditions in the Earth's interior.[7−10] Despite the importance, the coordination environments of framework cations ($^{[4]}Ge$, $^{[5]}Ge$) and their connectivity in GeO_2 and alkali germanate glasses are largely unknown.

Whereas the addition of network-modifying cations (e.g., Na^+, Mg^{2+}) in silicate glasses results in the formation of nonbridging oxygens (NBOs) without coordination transformation and the density increases with the Na content, the density (as well as the glass transition temperature, viscosity, and refractive index) of alkali germanate glasses exhibits maxima at around 15−20 mol % of the alkali oxide content: the density of Na_2O-GeO_2 glasses increases with Na content from about 3.8 g/cm^3 (for pure GeO_2 glasses) to about 4.05 g/cm^3 at the density maximum and then it decreases with further addition of Na. This is known as a *germanate anomaly*.[11] The atomic-scale origins of the anomaly are far from being understood. Earlier spectroscopic (Raman,[12−14] IR,[15] X-ray photoelectron spectroscopy,[16] NMR,[17,18] UV,[19] and X-ray absorption spectroscopy[20,21]) and scattering (X-ray and neutron[22]) studies have suggested seemingly different atomistic interpretations of the germanate anomaly, which include the formation of six-coordinated Ge,[11,17,18,20,22] the formation of a three-member ring,[12,13] or a medium-range order cluster linking a three-member ring and $^{[6]}Ge$.[23] Some of the discrepancies stem from the lack of unambiguous experimental evidence due to inherent disorder in germanate glasses. (Relevant reviews of experimental studies of germanate glasses and related controversies about the germanate anomaly can be found elsewhere.[13,23])

While the low sensitivity of ^{87}Ge (spin-$^7/_2$) NMR make it difficult to explore the coordination environment of Ge, the effective way to resolve the microscopic origin of the germanate anomaly is to explore the connectivity of the framework cations by probing bridging oxygen (BO) and NBO environments using ^{17}O NMR[24,25] (e.g., $^{[4]}Ge-O-^{[4]}Ge$, $Na-O-^{[4]}Ge$). A pioneering one-dimensional (1D) ^{17}O MAS NMR study of Na-germanate glasses[17,18] suggested the formation of $^{[6]}Ge-O-^{[4]}Ge$. Overlap among peaks under the 1D NMR technique, however, makes it difficult to make an unambiguous atomistic interpretation. The ^{17}O triple quantum (3Q) magic angle spinning (MAS) NMR has resolved the oxygen configurations in amorphous oxides by removing the second order quadrupolar interactions (e.g., refs 26−31) and can thus be effective in exploring the microscopic origins of the anomaly. Quantum chemical calculations are useful in obtaining NMR parameters in oxide glasses allowing us to assign previously unknown spectral features.[32] Quantum chemical calculations of the structurally relevant isotropic chemical shift of oxygen clusters (^{17}O δ_{iso}) in the germanate glasses have not been carried out so far. Here, we report the ^{17}O 3Q MAS NMR spectra for GeO_2 and Na-germanate glasses and results of quantum chemical calculations of the ^{17}O δ_{iso} that provide improved prospects for the atomistic origins of germanate anomaly.

2. Computational and Experimental Methods

Quantum chemical calculations were performed to establish the relationship between ^{17}O δ_{iso} and atomic configurations around BO using Gaussian98.[33] Clusters containing $^{[5]}Ge$ and $^{[4]}Ge$ ($Na^{[5]}Ge_4^{[4]}GeO_5(OH)_{11}$, $^{[5]}Ge$ cluster) and with $^{[6]}Ge$ ($Na^{[6]}Ge_4^{[4]}GeO_5(OH)_{12}$, $^{[6]}Ge$ cluster) were optimized at the Hatree−Fock level with a 6-311G(d) basis set. While we could not get an optimized configuration for a $Na^{[6]}Ge^{[4]}Si_4O_5(OH)_{12}$ cluster that satisfies Gaussian98's convergence criteria for both displacement and force, we chose a configuration satisfying convergence criteria for only force for NMR shielding tensor calculations. Chemical shielding tensors for oxygen clusters were calculated using the gauge-independent atomic orbital method

* Corresponding author. School of Earth and Environmental Sciences, Seoul National University, Seoul 151-742, Korea; sungklee@snu.ac.kr; phone, 82-2-880-6729; fax, 82-2-880-6729.

10.1021/jp063847b CCC: $33.50
Published on Web 07/29/2006

at the B3LYP level of theory and a 6-311G(2d,p) basis set for the optimized clusters.

GeO_2 and Na-germanate glasses ($(Na_2O)_x(GeO_2)_{1-x}$, X_{Na_2O} = 0, 0.167, and 0.33) were synthesized by fusing ^{17}O-enriched GeO_2 (prepared by hydrolyzing $Ge(OC_2H_5)_4$ with 40% ^{17}O enriched H_2O[17,18])−Na_2CO_3 mixtures at 1473−1673 K for 1 h in an Ar environment and quenching. As the maximum density in Na-germanate glasses is achieved at X_{Na_2O} of 0.15−0.2, $Na_2Ge_5O_{11}$ (X_{Na_2O} = 0.167) glass serves to explore the structural origins of the density maximum. If X_{Na_2O} is larger than 0.2, the formation of NBO was suggested[19] and thus $Na_2Ge_2O_5$ (X_{Na_2O} = 0.33) glass allows us to study the formation of NBO.

The ^{17}O Hahn echo and 3Q MAS NMR spectra were collected on a Bruker Avance 400 spectrometer (9.4 T) at a Larmor frequency of 54.22 MHz with a 4 mm triple-resonance probe. The recycle delay (RD) for the Hahn echo NMR experiments is 1 s with rf pulse lengths of 2.4 μs (a 90° tip angle) to 4.8 μs and an echo time of 1 ms. A ^{17}O 3Q MAS NMR spectrum was collected using a FAM-based shifted-echo pulse sequence[34] (5.5 μs−1 μs−20 μs) with a RD of 1 s. The sample spinning speed was 13 kHz for both experiments. The spectra are referenced to tap water with natural ^{17}O abundance.

3. Results and Discussion

Figure 1 shows the optimized model germanate cluster. The average $^{[4]}Ge-O$ bond length in the cluster is 1.726 Å and the $^{[5]}Ge-O$ and $^{[6]}Ge-O$ bond lengths are 1.760 and 1.801 Å, respectively. The average $^{[4]}Ge-O-^{[4]}Ge$ angle (141.5°) is larger than those for $^{[5]}Ge-O-^{[4]}Ge$ (130.7°) and $^{[6]}Ge-O-^{[4]}Ge$ (129.8°). The calculated ^{17}O δ_{iso} of $^{[5]}Ge-O-^{[4]}Ge$ (average chemical shielding of 216.0 ppm for O3, O17 and O21 in Figure 1) is larger than that of $^{[4]}Ge-O-^{[4]}Ge$ (average of 246.7 ppm for O2 and O11). The ^{17}O δ_{iso} difference between $^{[4]}Ge-O-^{[4]}Ge$ and $^{[5]}Ge-O-^{[4]}Ge$ clusters ranges from 26 to 35 ppm, The average chemical shielding for $^{[6]}Ge-O-^{[4]}Ge$ is 195.1 ppm and the ^{17}O δ_{iso} difference between $^{[4]}Ge-O-^{[4]}Ge$ and $^{[6]}Ge-O-^{[4]}Ge$ clusters ranges from 37 to 61.3 ppm (see Figure 1 caption for ^{17}O δ_{iso}, bond angle, and bond length of each oxygen cluster). The calculated results, therefore, show that ^{17}O δ_{iso} of $^{[n]}Ge-O-^{[4]}Ge$ increases with increasing n from 4 to 6, which is consistent with both the experimental and calculated trends for $^{[n]}Si$ (or Al)$-O-^{[4]}Si$ clusters where ^{17}O δ_{iso} increases with increasing n.[32]

Figure 2 shows ^{17}O Hahn echo NMR spectra for $(Na_2O)_x(GeO_2)_{1-x}$ glasses with varying X_{Na_2O}. The spectrum for GeO_2 glass (bottom) shows a typical quadrupolar pattern, consistent with the earlier 1D ^{17}O MAS NMR spectrum.[18] As X_{Na_2O} increases from 0 to 0.167, the peak positions move to a higher frequency and then move to a lower frequency with a further increase in X_{Na_2O} up to 0.33. The clear structural origins of these changes, however, cannot be uniquely determined from 1D NMR spectra because of the overlap among possible oxygen sites in germanate glasses and the large quadrupolar coupling constant (C_q) of oxygen clusters (about 7 MHz).[17,18]

Figure 3 presents the ^{17}O 3Q MAS NMR spectra for $(Na_2O)_x(GeO_2)_{1-x}$ glasses with varying X_{Na_2O} where at least three oxygen clusters are resolved. An ^{17}O 3QMAS NMR spectrum for GeO_2 glasses (Figure 3 bottom) shows a single $^{[4]}Ge-O-^{[4]}Ge$ peak (around −64 ppm in the isotropic dimension). The spectrum for Na-germanate glasses at X_{Na_2O} = 0.33 (Figure 3 top) exhibits a $^{[4]}Ge-O-^{[4]}Ge$ peak and a new peak around −49 ppm in the isotropic dimension that corresponds to the NBO peak ($Na-O-^{[4]}Ge$) as expected from the composition. The ^{17}O 3Q MAS NMR spectrum for X_{Na_2O} = 0.167 glasses shows both a $^{[4]}Ge-O-^{[4]}Ge$ cluster and $Na-O-^{[4]}Ge$ but it also reveals an additional peak at around −80 to −95 ppm in the isotropic dimension. This peak is likely to correspond to $^{[6,5]}Ge-O-^{[4]}Ge$. This peak assignment is based on the above quantum chemical calculations (see below for further discussion), consistent with the correlation established for silicates.[32] The current result demonstrates the formation of both $^{[6,5]}Ge-O-^{[4]}Ge$ and $Na-O-^{[4]}Ge$ at a density maximum.

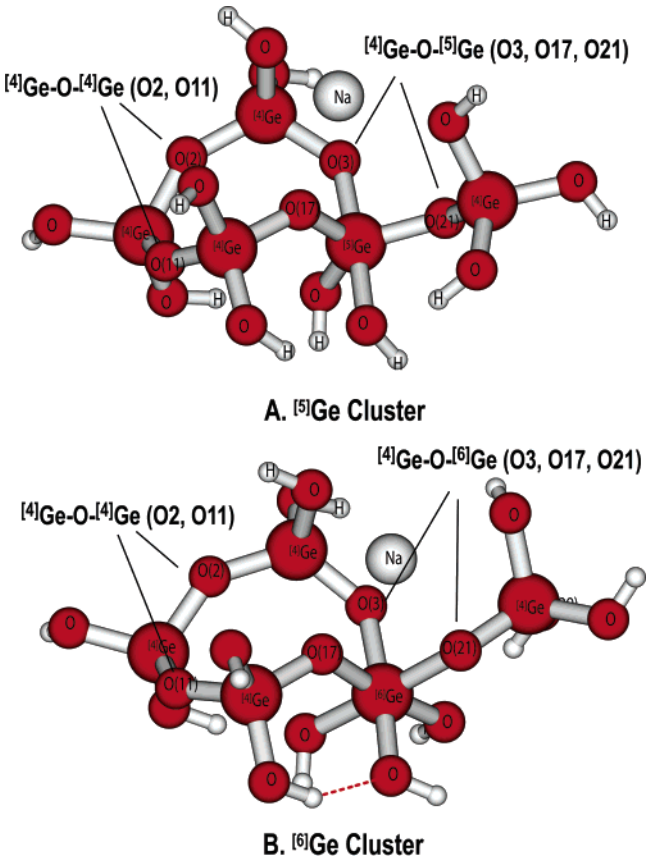

Figure 1. (A) The optimized geometry of bridging oxygen clusters ($Na^{[4]}Ge_4^{[5]}GeO_5(OH)_{11}$) with $^{[5]}Ge$. O(3), O(17), and O(21) are oxygen linking $^{[5]}Ge$ and $^{[4]}Ge$ ($^{[5]}Ge-O-^{[4]}Ge$) and O(4) and O(5) are $^{[4]}Ge-O-^{[4]}Ge$. The average bond length [($^{[5]}Ge-O$ + $^{[4]}Ge-O$)/2], angles (Ge−O−Ge), and chemical shielding are [1.772 Å, 133.4°, and 207.3 ppm] respectively for O(3); [1.767 Å, 129.7°, and 217.6 ppm] for O(17); [1.741 Å, 128.8°, and 221.4 ppm] for O(21). For $^{[4]}Ge-O-^{[4]}Ge$ clusters, these are [1.727 Å, 147.1°, and 250.8 ppm] for O(2); [1.727 Å, 142.3°, and 246.4 ppm] for O(11). (B) The optimized geometry (see computational and experimental methods for simulation details) of bridging oxygen clusters ($Na^{[4]}Ge_4^{[6]}GeO_5(OH)_{11}$) with $^{[6]}Ge$. O(3), O(17), and O(21) are oxygen linking $^{[6]}Ge$ and $^{[4]}Ge$ ($^{[6]}Ge-O-^{[4]}Ge$) and O(4) and O(5) are $^{[4]}Ge-O-^{[4]}Ge$. The average bond lengths (($^{[6]}Ge-O$ + $^{[4]}Ge-O$)/2), angles (Ge−O−Ge), and chemical shielding are 1.802 Å, 131.7°, and 188.5 ppm, respectively, for O(3); 1.811 Å, 126.2°, and 189.2 ppm for O(17); and 1.791 Å, 129.4°, and 207.7 ppm for O(21). For $^{[4]}Ge-O-^{[4]}Ge$ clusters, these are 1.731 Å, 141.7°, and 244.8 ppm for O(2) and 1.730 Å, 123.3°, and 249.8 ppm for O(11).

Figure 4A shows the isotropic projections of the ^{17}O 3Q MAS NMR spectra for the glasses on the $GeO_2-Na_2Ge_2O_5$ join. The approximate value of ^{17}O δ_{iso} and the C_q (with estimated asymmetry parameter of η of 0.5, similar to the results from the earlier 1D MAS NMR[17,18]) were estimated from the peak positions (for $Na_2Ge_5O_{11}$ glass) and the centers of gravity of the peaks (for GeO_2 and $Na_2Ge_2O_5$ glasses).[35] The ^{17}O δ_{iso} for $^{[4]}Ge-O-^{[4]}Ge$ varies from 44.7 ± 3 ppm (with a C_q of 7.4 ± 0.2 MHz at an η of 0.5 for GeO_2 glass), 62.8 ± 3 ppm (with a C_q of 6.6 ± 0.2 MHz at an η of 0.5 for X_{Na_2O} = 0.167 glass), to 68.0 ± 3 ppm (with a C_q of 6.3 ± 0.2 MHz at an η of 0.5

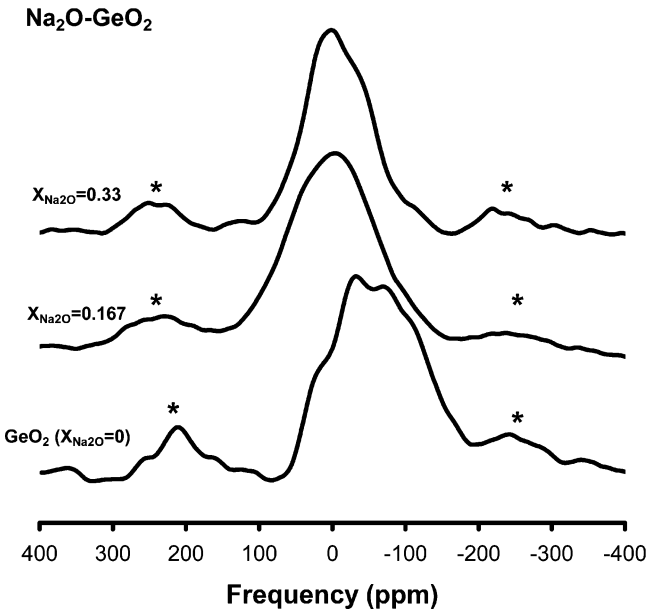

Figure 2. ^{17}O Hahn echo NMR spectra for $(Na_2O)_x(GeO_2)_{1-x}$ glasses with varying x (from 0, 0.17, to 0.33) as labeled. * refers to spinning side bands.

for $X_{Na_2O} = 0.33$ glass). Note that the ^{17}O δ_{iso} for $^{[4]}$Ge−O−$^{[4]}$Ge is smaller than that reported from previous 1D NMR spectra (about 70 ppm).[17] This discrepancy may be due to the rather large C_q values of oxygen clusters, making it difficult to obtain reliable NMR parameters with 1D NMR techniques in relatively low magnetic fields (e.g., below 9.4 T) as previously demonstrated.[36] The ^{17}O δ_{iso} for $^{[4]}$Ge−O−$^{[4]}$Ge increases with increasing Na content, mostly due to an increase in the Ge−NBO bond length with X_{Na_2O}.

The ^{17}O δ_{iso} for the new peak at −85 ppm in the isotropic dimension in $X_{Na_2O} = 0.167$ glass is estimated to be about 97.8 ± 5 ppm (with a C_q of 6.5 ± 0.4 MHz at an η of 0.5). The ^{17}O δ_{iso} difference between $^{[4]}$Ge−O−$^{[4]}$Ge and $^{[5]}$Ge−O−$^{[4]}$Ge in Na-germanate is about 29−35 ppm, showing a remarkable similarity with the difference between $^{[5]}$Ge−O−$^{[4]}$Ge and $^{[4]}$Ge−O−$^{[4]}$Ge calculated using quantum chemical calculations, and, thus, confirms the formation of highly coordinated Ge at the density maximum. Our preliminary quantum chemical calculations also showed that an increase in Ge−O bond length in $^{[4]}$Ge−O−$^{[4]}$Ge cluster of about 0.3 Å without Ge coordination transformation corresponds to an increase in ^{17}O δ_{iso} of about 7.5 ppm. The peak near −85 ppm (about 32 ppm deshileded from $^{[4]}$Ge−O-$^{[4]}$Ge) in the isotropic dimension, therefore, cannot be due to the formation of small member ring cluster (i.e., three-member ring) but it must stem from highly coordinated Ge (i.e., $^{[5]}$Ge). It should also be noted that there is a significant intensity in the peak near −90 to −95 ppm of the isotropic dimension. The estimated ^{17}O δ_{iso} for the feature ranges about 110−120 ppm and is about 40−60 ppm deshielded from $^{[4]}$Ge−O−$^{[4]}$Ge. This ^{17}O δ_{iso} difference is consistent with the calculated difference between $^{[4]}$Ge−O−$^{[4]}$Ge and $^{[6]}$Ge−O−$^{[4]}$Ge and implies the formation of a nonnegligible amount of $^{[6]}$Ge at the density maximum.

The current experimental data also show that ^{17}O C_q of the $^{[4]}$Ge−O−$^{[4]}$Ge cluster apparently decreases with Na content from pure GeO_2 (about 7.4 MHz) to $X_{Na_2O} = 0.33$ (about 6.33 MHz) glasses. Recent quantum chemical calculations showed that ^{17}O C_q of simple $^{[4]}$Ge−O−$^{[4]}$Ge cluster with a charge-balancing Na cation increases with increasing bond angle and alkali metal−oxygen distance.[37,38] The current result, therefore,

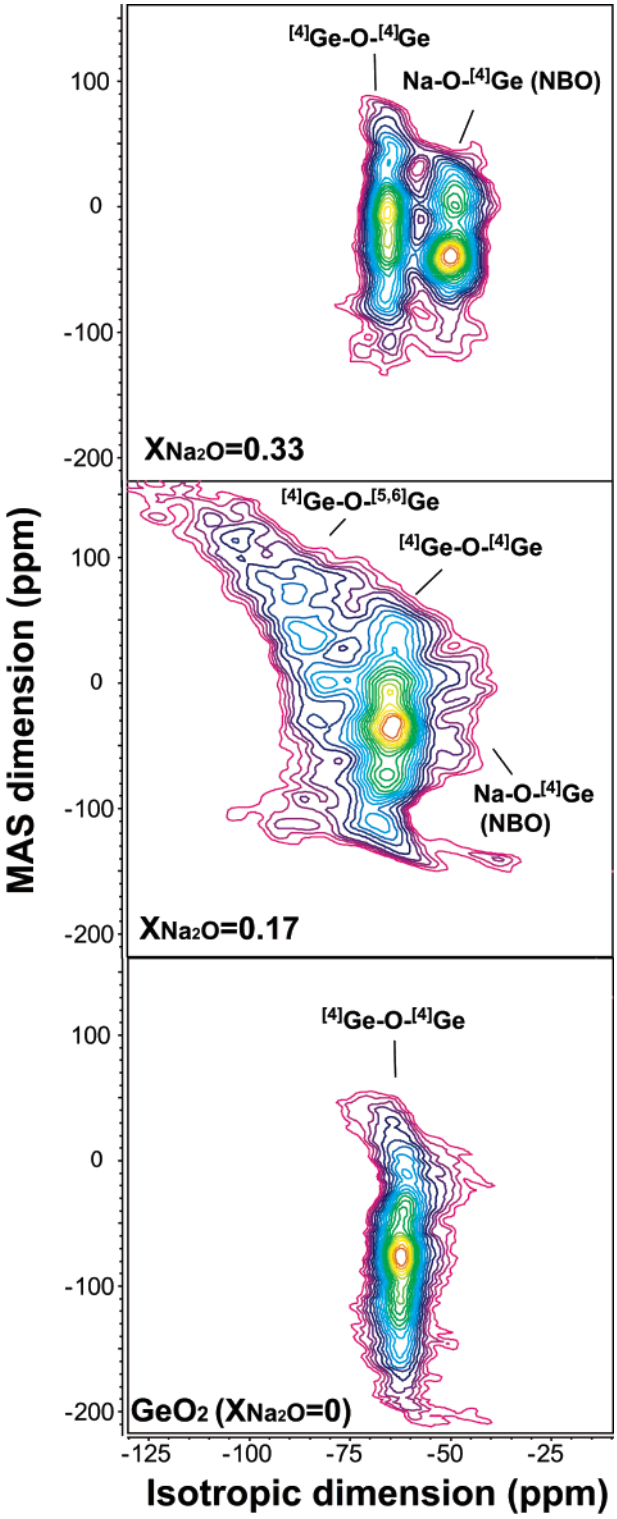

Figure 3. ^{17}O 3Q MAS NMR spectra for $(Na_2O)_x(GeO_2)_{1-x}$ glasses with varying x as labeled. Contour lines are drawn from 13% to 93% of the relative intensity with a 5% increment and added lines at 4, 7, and 10%.

suggests that the $^{[4]}$Ge−O−$^{[4]}$Ge bond angle and Na−O distances decrease with increasing Na content in the Na-germanate glasses. The ^{17}O δ_{iso} and C_q for Na−O−$^{[4]}$Ge are 48.9 ± 3 ppm and 5.5 ± 0.2 MHz (with η of 0.5), respectively. We note that while future quantum chemical calculations will reveal the detailed relationship between ^{17}O C_q and atomic configurations in the larger clusters, our preliminary quantum chemical calculations using Ge−O−Ge cluster (instead of ring

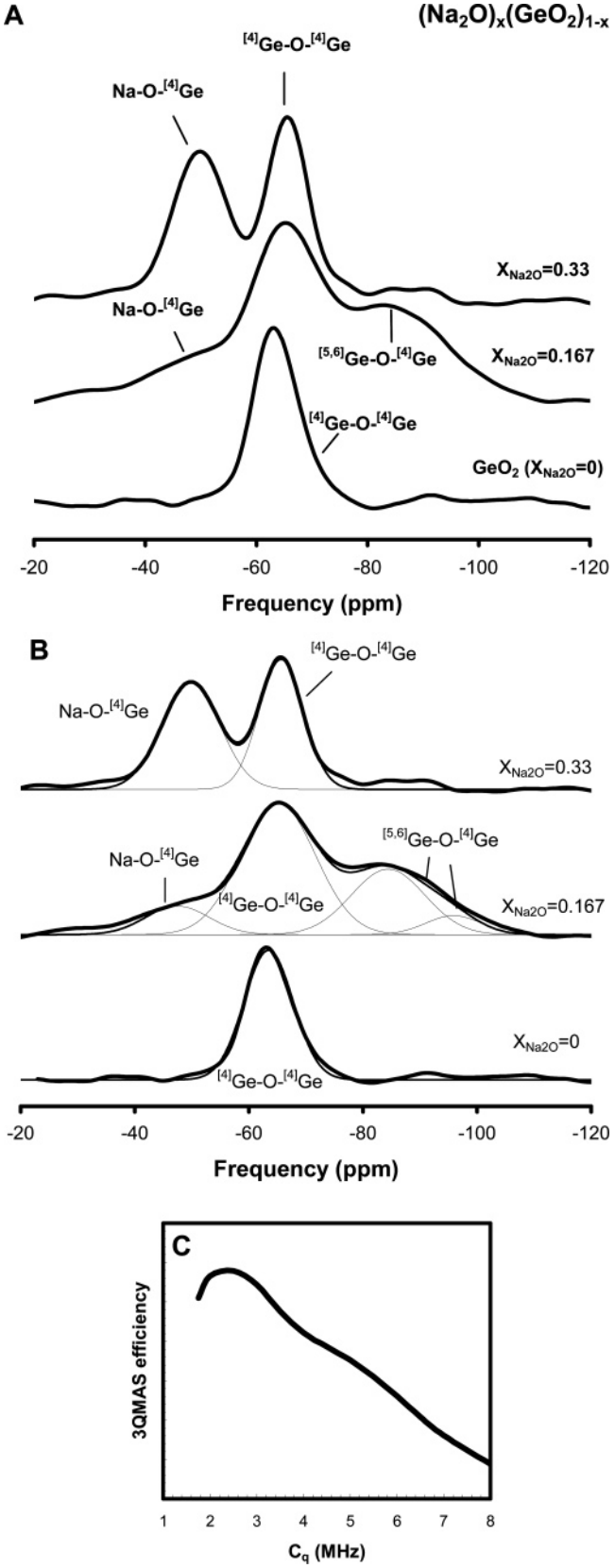

Figure 4. (A) Isotropic projection of ^{17}O 3Q MAS NMR spectra of $(Na_2O)_x(GeO_2)_{1-x}$ glasses with varying x as labeled. (B) Fitting result of ^{17}O 3Q MAS NMR spectra using Gaussian functions (thin lines). Thick lines refer to the experimental ^{17}O 3Q MAS NMR spectra. (C) Calculated dependence of triple-quantum magic-angle spinning (3Q MAS) efficiency on C_q using the Simpson[41] for spin $^5/_2$ nuclei with η of 0.5. Radio frequency field strength is 70 kHz, and all the simulation conditions are equivalent to the experimental setup for the current study.

cluster used here) show that C_q for $^{[n]}$Ge−O−$^{[4]}$Ge slightly increases with n from 4 to 6.

Figure 4B shows fitting (and simulation for $X_{Na_2O} = 0.167$ glass) results of the isotropic projection of 3Q MAS NMR spectra using Gaussian functions representing NBO and BO clusters. The $^{[5,6]}$Ge−O−$^{[4]}$Ge peak was decomposed into two Gaussian parts corresponding to $^{[5]}$Ge−O−$^{[4]}$Ge and $^{[6]}$Ge−O−$^{[4]}$Ge in the $X_{Na_2O} = 0.167$ glass, while further compositional effects remain to be explored. The ^{17}O δ_{iso} distribution for the $^{[4]}$Ge−O−$^{[4]}$Ge (with a fwhm of 15.4 ppm) and a Na−O−$^{[4]}$Ge cluster (a fwhm of 14.6 ppm) in the $X_{Na_2O} = 0.167$ glass, manifested by the width of the isotropic dimension in the ^{17}O 3Q MAS NMR spectra, are much larger than those for oxygen clusters in GeO_2 and $X_{Na_2O} = 0.33$ glasses (a fwhm of 9−10 ppm for $^{[4]}$Ge−O−$^{[4]}$Ge and 12.0 ppm for Na−O−$^{[4]}$Ge) (Figure 2). The result implies larger topological disorder due to an increase in bond length and angle distribution for $X_{Na_2O} = 0.167$ glass: the width of oxygen cluster peak of the 3Q MAS dimension is dependent on the distribution of the second-order quadrupolar shift (and thus C_q) as well as δ_{iso}. The peak position in both the 3Q MAS and the MAS dimension allows us to yield a relationship between C_q and δ_{iso} of $^{[4]}$Ge−O−$^{[4]}$Ge (see, refs 35,39, and 40 for more details). The distribution of C_q and δ_{iso} of $^{[4]}$Ge−O−$^{[4]}$Ge cluster in the pure GeO_2 and $X_{Na_2O} = 0.33$ glasses are rather positively correlated. Whereas it is difficult to directly obtain the relationship between ^{17}O C_q and δ_{iso} for the oxygen clusters in the $X_{Na_2O} = 0.167$ glasses due to peak overlap, the widths for oxygen clusters (particularly, $^{[4]}$Ge−O−$^{[4]}$Ge) in the isotropic dimension are also likely due to variations in both C_q and δ_{iso}, suggesting wider bond angle and length distribution. We note that a similar trend of increasing topological entropy upon densification has been observed for silicate glasses at high pressure.[32] The $^{[5,6]}$Ge−O−$^{[4]}$Ge peak also shows wide distributions of chemical shift and the second-order quadrupolar shift, implying significant configurational and topological disorder.

The oxygen cluster population allows us to estimate the extent of mixing of framework and nonframework cations.[32] Because the MQMAS NMR signal intensity is dependent on the characteristics of oxygen sites (e.g., C_q) and experimental conditions (mostly the rf power of pulses), the fractions of oxygen clusters were theoretically calibrated considering a C_q dependence of 3Q efficiency at η of 0.5[41] (see Figure 4C for calculated 3Q MAS efficiency with C_q): simulation results show that 3Q efficiency decreases almost linearly with increasing C_q (from 5 to 7.5 MHz). The calibrated proportion of $^{[4]}$Ge−O−$^{[4]}$Ge varies from 100% (pure GeO_2), to about 58.9 ± 2.5% ($X_{Na_2O} = 0.167$) and 52.7 ± 2.5% ($X_{Na_2O} = 0.33$). The fraction of $^{[5,6]}$Ge−O−$^{[4]}$Ge in $X_{Na_2O} = 0.167$ glass is about 34.1 ± 2.5% (including about 5.7% of $^{[6]}$Ge−O−$^{[4]}$Ge). Note that pure GeO_2 and $X_{Na_2O} = 0.33$ glass do not have $^{[5,6]}$Ge−O−$^{[4]}$Ge. The proportion of NBO (Na−O−$^{[4]}$Ge) increases from 0% (pure GeO_2), to about 7 ± 2% ($X_{Na_2O} = 0.167$) and 47.3 ± 2.5% ($X_{Na_2O} = 0.33$). Assuming a $^{[5]}$Ge/$^{[6]}$Ge ratio of 7/3 and a chemical order (favoring complete mixing among framework units), our quasi-chemical approximation[24] shows the formation of about 38% of $^{[5,6]}$Ge−O−$^{[4]}$Ge (similar with about 34% from the experiment).

While there is no definite evidence for the formation of a three-member ring in ^{17}O NMR spectra, the larger dispersion of the chemical shift in the $^{[4]}$Ge−O−$^{[4]}$Ge in the $X_{Na_2O} = 0.167$ glass stems from the variation of the $^{[4]}$Ge−O bond length and thus the ring topology, which could include a smaller member ring as previously suggested.[12,13] The densification mechanism

related to the observed oxygen cluster population can be described by the following two schemes. In the range of X_{Na_2O} up to the density maximum considering the formation of a small-member ring, the coordination transformation, topological variations (e.g. formation of small ring cluster) as well as NBO can account for densification

$$^{[4]}Ge-O-^{[4]}Ge + Na_2O \Rightarrow \text{small ring cluster } (^{[4]}Ge) + {}^{[4]}Ge-O-^{[5,6]}Ge + M-O-^{[4]}Ge \quad (1)$$

where M is an alkali cation. At the higher X_{Na_2O} content, the following scheme serves to describe the greatest changes in the oxygen cluster population:

$$Na_2O + \text{small ring } (^{[4]}Ge) + {}^{[5,6]}Ge \Rightarrow M-O-^{[4]}Ge \quad (2)$$

These schemes are similar to our earlier observations of an increase in the boroxol ring concentration in v-B_2O_3 with a pressure of up to about 2 GPa and a subsequent decrease in boroxol ring fraction with a pressure above 6 GPa upon forming $^{[4]}B$ as reported from our NMR and inelastic X-ray scattering studies.[42,43] We also note that while coordination transformation would be the important control of density of oxide glasses, the variations in medium range order and topological variation play an important role in determining the density of several oxide glasses including alkali borate and phosphate glasses (e.g., refs 44 and 45). The current experimental results for alkali−germanate glasses demonstrate that both contributions (coordination transformation and topological rearrangement) are responsible for the densification and the germinate anomaly, yielding improved prospects for atomistic origins and the nature of densification in alkali germanate glasses.

In summary, 2D ^{17}O NMR with much improved resolution, in conjunction with quantum chemical calculations, allow us to obtain structural details and framework connectivity in the germanate glasses, which includes the formation of both NBO and $^{[5,6]}Ge-O-^{[4]}Ge$ in Na_2O-GeO_2 glasses near the density maximum. Composition-induced densification is also accompanied by an increase in topological disorder, providing atomistic constraints for germanate anomaly. These mechanisms are also remarkably similar to pressure-induced structural changes in the other archetypal glass-forming liquids, yielding insights into more complete understanding of the macroscopic properties of archetypal glasses, and the nature of densification in the oxide glasses in general.

Note Added in Proof: O17 2-dimensional NMR spectra for NA-germanate glasses with similar compositions at higher magnetic fields (14.1 and 18.8 T) were recently published.[46] Their NMR peak assignment and results are consistent with the results presented here based both on NMR and quantum chemical calculations.

Acknowledgment. This research is supported by the Korea Research Foundation (C00076) to S. K. Lee. We thank Professor Grandinetti for RMN software for 2D NMR data processing.

References and Notes

(1) Elliot, S. R. *Physics of amorphous materials*; John Wiley & Sons: New York, 1988.
(2) Lee, S. K.; Stebbins, J. F. *J. Phys. Chem. B* **2000**, *104*, 4091.
(3) Mysen, B. O.; Richet, P. *Silicate Glasses and Melts*: *Properties and Structure*; Elsevier: Amsterdam, 2005.
(4) Navrotsky, A.; Peraudeau; McMillan, P.; Coutures, J. P. *Geochim. Cosmochim. Acta* **1982**, *46*, 2039.
(5) Sen, S.; Stebbins, J. F. *Phys. Rev. B* **1997**, *55*, 3512.
(6) Meyer, A.; Schober, H.; Neuhaus, J. *Phys. Rev. B* **2001**, *6321*.
(7) Merkel, S.; Kubo, A.; Miyagi, L.; Speziale, S.; Duffy, T. S.; Mao, H. K.; Wenk, H. R. *Science* **2006**, *311*, 644.
(8) Guthrie, M.; Tulk, C. A.; Benmore, C. J.; Xu, J.; Yarger, J. L.; Klug, D. D.; Tse, J. S.; Mao, H. K.; Hemley, R. J. *Phys. Rev. Lett.* **2004**, *93*.
(9) Sugai, S.; Onodera, A. *Phys. Rev. Lett.* **1996**, *77*, 4210.
(10) Trachenko, K.; Dove, M. T.; Brazhkin, V.; El'kin, F. S. *Phys. Rev. Lett.* **2004**, *93*.
(11) Murthy, M. K.; J., I. *Nature* **1964**, *201*, 285.
(12) Henderson, G. S.; Amos, R. T. *J. Non-Cryst. Solids* **2003**, *328*, 1.
(13) Henderson, G. S.; Wang, H. M. *Eur. J. Mineral.* **2002**, *14*, 733.
(14) Di Martino, D.; Santos, L. F.; Marques, A. C.; Almeida, R. M. *J. Non-Cryst. Solids* **2001**, *293*, 394.
(15) Kamitsos, E. I.; Yiannopoulos, Y. D.; Jain, H.; Huang, W. C. *Phys. Rev. B* **1996**, *54*, 9775.
(16) Di Martino, D.; Santos, L. F.; Almeida, R. M.; Montemor, M. F. *Surf. Interface Anal.* **2002**, *34*, 324.
(17) Hussin, R.; Dupree, R.; Holland, D. *J. Non-Cryst. Solids* **1999**, *246*, 159.
(18) Hussin, R.; Holland, D.; Dupree, R. *J. Non-Cryst. Solids.* **1998**, *232−234*, 440.
(19) Trukhin, A. N.; Kulis, P. *J. Non-Cryst. Solids.* **1995**, *188*, 125.
(20) Huang, W. C.; Jain, H.; Meitzner, G. *J. Non-Cryst. Solids* **1996**, *196*, 155.
(21) Wang, H. M.; Henderson, G. S. *Chem. Geol.* **2004**, *213*, 17.
(22) Hoppe, U.; Kranold, R.; Weber, H. J.; Neuefeind, J.; Hannon, A. C. *J. Non-Cryst. Solids* **2000**, *278*, 99.
(23) Yiannopoulos, Y. D.; Varsamis, C. P. E.; Kamitsos, E. I. *Chem. Phys. Lett.* **2002**, *359*, 246.
(24) Lee, S. K.; Fei, Y.; Cody, G. D.; Mysen, B. O. *Geophys. Res. Lett.* **2003**, *30*, 1845.
(25) Lee, S. K.; Mysen, B. O.; Cody, G. D. *Phys. Rev. B* **2003**, *68*, 214206.
(26) Dirken, P. J.; Kohn, S. C.; Smith, M. E.; Vaneck, E. R. H. *Chem. Phys. Lett.* **1997**, *266*, 568.
(27) Stebbins, J. F.; Xu, Z. *Nature* **1997**, *390*, 60.
(28) Lee, S. K.; Musgrave, C. B.; Zhao, P.; Stebbins, J. F. *J. Phys. Chem. B* **2001**, *105*, 12583.
(29) Amoureux, J.-P.; Bauer, F.; Ernst, H.; Fernandez, C.; Freude, D.; Michel, D.; Pingel, U.-T. *Chem. Phys. Lett.* **1998**, *285*.
(30) Frydman, I.; Harwood, J. S. *J. Am. Chem. Soc.* **1995**, *117*, 5367.
(31) Massiot, D.; Touzo, B.; Trumeau, D.; Coutures, J. P.; Virlet, J.; Florian, P.; Grandinetti, P. J. *Solid State NMR* **1996**, *6*, 73.
(32) Lee, S. K. *J. Phys. Chem. B* **2004**, *108*, 5889.
(33) Frisch, M. J.; Trucks, G. W.; Schlegel, H. B.; Scuseria, G. E.; Robb, M. A.; Cheeseman, J. R.; Zakrzewski, V. G.; Montgomery, J. A., Jr.; Stratmann, R. E.; Burant, J. C.; Dapprich, S.; Millam, J. M.; Daniels, A. D.; Kudin, K. N.; Strain, M. C.; Farkas, O.; Tomasi, J.; Barone, V.; Cossi, M.; Cammi, R.; Mennucci, B.; Pomelli, C.; Adamo, C.; Clifford, S.; Ochterski, J.; Petersson, G. A.; Ayala, P. Y.; Cui, Q.; Morokuma, K.; Malick, D. K.; Rabuck, A. D.; Raghavachari, K.; Foresman, J. B.; Cioslowski, J.; Ortiz, J. V.; Stefanov, B. B.; Liu, G.; Liashenko, A.; Piskorz, P.; Komaromi, I.; Gomperts, R.; Martin, R. L.; Fox, D. J.; Keith, T.; Al-Laham, M. A.; Peng, C. Y.; Nanayakkara, A.; Gonzalez, C.; Challacombe, M.; Gill, P. M. W.; Johnson, B. G.; Chen, W.; Wong, M. W.; Andres, J. L.; Head-Gordon, M.; Replogle, E. S.; Pople, J. A. *Gaussian 98*, Revision A.11; Gaussian, Inc.: Pittsburgh, PA, 1998.
(34) Madhu, P. K.; Goldbourt, A.; Frydman, L.; Vega, S. *Chem. Phys. Lett.* **1999**, *307*, 41.
(35) Baltisberger, J. H.; Xu, Z.; Stebbins, J. F.; Wang, S.; Pines, A. *J. Am. Chem. Soc.* **1996**, *118*, 7209.
(36) Lee, S. K.; Stebbins, J. F.; Weiss, C. W.; Kirkpatrick, R. J. *Chem. Mater.* **2003**, *15*, 2605.
(37) Clark, T. M.; Grandinetti, P. J. *J. Non-Cryst. Solids* **2000**, *265*, 75.
(38) Clark, T. M.; Grandinetti, J. *Solid State NMR* **2000**, *16*, 55.
(39) Lee, S. K.; Stebbins, J. F. *Geochim. Cosmochim. Acta* **2003**, *67*, 1699.
(40) Angeli, F.; Charpentier, T.; Faucon, P.; Petit, J. C. *J. Phys. Chem. B* **1999**, *103*, 10356.
(41) Bak, M.; Rasmussen, J. T.; Nielsen, N. C. *J. Magn. Reson.* **2000**, *147*, 296.
(42) Lee, S. K.; Eng, P. J.; Mao, H. K.; Meng, Y.; Newville, M.; Hu, M. Y.; Shu, J. F. *Nat. Mater.* **2005**, *4*, 851.
(43) Lee, S. K.; Mibe, K.; Fei, Y.; Cody, G. D.; Mysen, B. O. *Phys. Rev. Lett.* **2005**, *94*, 165507.
(44) Tischendorf, B. C.; Alam, T. M.; Cygan, R. T.; Otaigbe, J. U. *J. Non-Cryst. Solids.* **2003**, *316*, 261.
(45) Bray, P. J. *J. Non-Cryst. Solids* **1985**, *73*, 19.
(46) Du, L. S.; Stebbins, J. F. *J. Phys. Chem. B* **2006**, *110*, 12427.